Optical-bias effects in electron-drift measurements and defect relaxation in a-Si:H

Daxing Han

Department of Physics, University of North Carolina, Chapel Hill, North Carolina 27599-3255

Douglas C. Melcher and E. A. Schiff

Department of Physics, Syracuse University, Syracuse, New York 13244-1130

M. Silver

Department of Physics, University of North Carolina, Chapel Hill, North Carolina 27599-3255

(Received 20 November 1992; revised manuscript received 22 June 1993)

We report measurements of the effects of optical bias upon photocharge transients in a-Si:H. Transients were recorded from 100 ns to 10 s following a laser pulse. Without optical bias these transients exhibit a form consistent with trapping of electrons by a deep level; this result is consistent with extensive prior research. However, even low levels of optical bias (generation rate 10^{17} cm^{-3}s^{-1}) suppress deep trapping, leading to an enhancement of electron drift by as much as one decade. We propose that charge state transitions associated with optical bias leave defects in metastable configurations. The corresponding transition energies lie closer to the conduction band than for the defect's relaxed, equilibrium configuration.

I. INTRODUCTION

It has slowly become clearer in the last several years that a conventional approach to studying excess carrier drift and recombination in hydrogenated amorphous silicon is disappointing in its range of successful predictions. In this conventional approach one divides a density of one-electron states into bands: transport states, traps, and recombination centers. Experiments are viewed largely as determining this density of states and the transport and kinetic parameters (mobilities, capture coefficients, etc.) of the bands.

This is not to say that the conventional approach has not enjoyed considerable success in a-Si:H. In particular many electron drift measurements done using photocarrier techniques under near dark conditions (time-of-flight,[1-6] charge collection,[1,7,8] modulated photocurrent,[9-12] and transient photocurrent and photocharge[13-15]) are broadly consistent with the view illustrated in Fig. 1.[15] The upper panel of the figure illustrates the average displacement (or *drift*) $x(t)$ of a photogenerated electron in an electric field F as a function of time t following generation. There are four domains.

(1) A short time domain lasting to about 10^{-7} s in which the electron moves fairly rapidly; this is usually studied using the time-of-flight method.

(2) An intermediate "plateau" ($10^{-6} - 10^{-4}$ s) in which the additional displacement is small; this is usually examined using the charge collection method.

(3) A subsequent long-time domain (10^{-3}–1 s) in which the electron's displacement again increases significantly.

(4) A terminal plateau at times greater than about 10 s. These last two regimes are studied using transient photocurrent techniques without carrier sweepout.

The lower panel illustrates a density of states used for a conventional analysis; the two distinct bands are a band-tail, which rises monotonically towards the conduction band edge E_C, and a deep level. The temporal domains are associated with (i) band-tail multiple trapping; (ii)
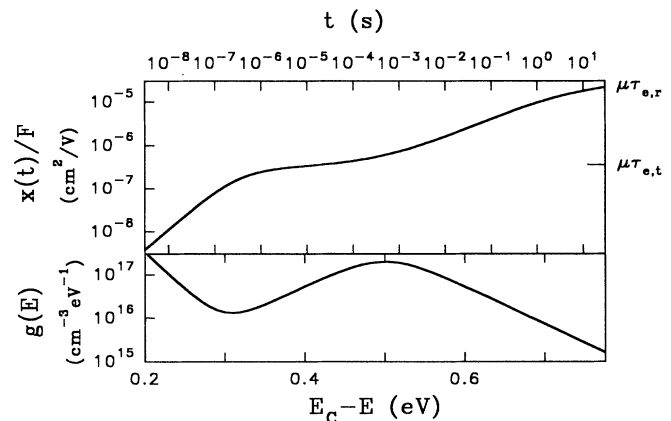

FIG. 1. The upper panel indicates the drift of an electron in a-Si:H suggested by transient photocurrent measurements. In particular the ratio $x(t)/F$ of the displacement $x(t)$ to the electric field F is shown as a function of the time delay t following photogeneration. Note that the average drift mobility of the carrier for early times $[x(t)/Ft]$ is about $\mu = 1$ cm^2/Vs. The deep-trapping and recombination mobility lifetime products $\mu\tau_{e,t}$ and $\mu\tau_{e,r}$ which can be estimated from such measurements are also indicated. The lower panel is a density of states which accounts for these measurements invoking an exponential band tail and a deep level 0.5 eV below the band-edge.

trapping by the deep level; (iii) multiple trapping with the deep level; and (iv) recombination.

The reason we said that this picture is disappointing is that it does not readily account for measurements under different conditions. We include in this list of measurements steady-state photoconductivity,[16–19] steady-state space-charge limited current,[20,21] transient photocurrents measured under optical bias,[22–27] and transient space-charge limited currents.[28,29] Broadly speaking, these measurements do not indicate any well defined deep trapping process, and thus do not usually suggest the structured form of the density of states with a distinct defect level as indicated in Fig. 1.

We have undertaken a series of measurements which we believe elucidate this dilemma. In particular we report our measurements of optical-bias effects on the displacement of electron photocarriers in a-Si:H recorded following a laser illumination pulse. We employed the transient photocharge technique; our results extend recent work using the method without optical bias.[15,30–32] In brief, we observed an *enhancement* of electron drift due to optical bias. This effect has been reported before.[22,23,27] In the present work we have expanded the temporal range over which the effect is measured by several orders or magnitude; it is now clear that the optical-bias enhancement is due to suppression of deep-trapping.

This type of effect is usually addressed using occupancy changes of deep levels (quasi-Fermi-level motion). We shall argue that this model is unsatisfactory, and that the most probable physical mechanism for suppression of deep trapping is metastable configurations of the deep level. These would effectively move the level to shallower energies under optical bias than in the dark. Defect relaxation has also been invoked to account for optical-bias effects on the spin relaxation of the D center in undoped a-Si:H.[33] Perhaps the strongest evidence for relaxation processes is recent capacitance transient research in a-Si:H,[34–36] which indicates that the level deepens logarithmically in time following filling with electrons.

We shall not discuss microscopic mechanisms for level shifts in this paper. Branz and Schiff[37] have suggested elsewhere that the magnitudes are consistent with previous theoretical estimates of relaxation for the D center, although the logarithmic time dependence remains unexplained.

II. EXPERIMENTAL PROCEDURES

All measurements in this paper were done at room temperature. We measured optical-bias effects in three specimens. The qualitative effects were comparable, and we shall report the results for only one specimen. This specimen is an undoped, 3.3×10^{-4} cm thick a-Si:H layer on a Corning, Inc. type 7059 glass substrate deposited at Syracuse University. The spin density in the annealed state was $3 \times 10^{15} \text{cm}^{-3}$. Coplanar chromium electrodes were evaporated onto the specimen's surface. The gap w between the electrodes was 0.5 mm; the length of the electrodes was $l = 1$ cm.

Transient photocharge measurements were done at Syracuse University using the apparatus described in some detail previously.[15] We show the schematic design of this apparatus in Fig. 2. A dc bias voltage is applied to the specimen electrodes. The dc current through the specimen is sunk into a constant current source.

We performed two tests to check whether the electric field in the specimen is uniform. First, both dc and transient currents were reasonably proportional to the applied bias voltage. Second, we measured the charge which flowed out of the specimen immediately after the bias voltage is returned to zero. We observed only the charge expected from the geometrical capacitance of the electrode structure. This is essentially a definitive test for field uniformity, since nonuniformity requires that a significant excess space-charge be stored in the specimen between its electrodes. A more complete description is given elsewhere.[30]

When a laser pulse is absorbed by the specimen, a transient current flows onto an integrating capacitor; the transient voltage on this capacitor is recorded using a digital oscilloscope and subsequently converted into a transient photocharge $Q(t)$. We recorded data over the range $10^{-8} - 10^{1}$ s; this large range required that we take the data in three time sections using different amplifiers, integrating filters, and oscilloscope settings.

The transients reported here were generated with a laser wavelength of 630 nm; the pulse width of the laser is about 3 ns. The laser beam was broadened with a lens to uniformly illuminate the specimen area between the electrodes. We calibrated the incident intensity of the laser using a commercial Si p-i-n diode photodetector.

Our procedure for normalizing the transient photocharge and photocurrent measurements requires an estimate of the photocharge Q_0 of electrons and holes photogenerated in the specimen by the laser. This magnitude is readily computed from the laser intensity, since essentially all photons which entered the specimen would be absorbed at the laser wavelength. Earlier work has
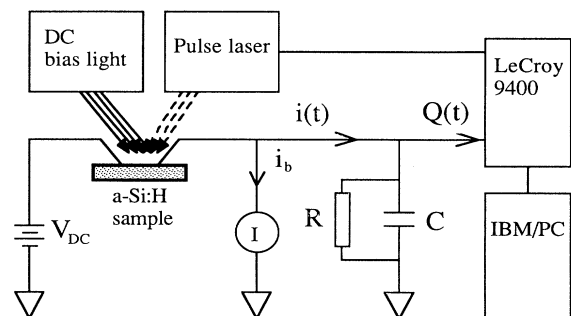

FIG. 2. Block diagram of transient photocurrent/ photocharge apparatus. A dc voltage bias is applied to the specimen; the resulting steady-state current is sunk into the current source I_{SS}. The transient photocurrent $i(t)$ passes through an RC filter; the output voltage $V(t)$ was typically recorded for times $t \ll RC$, and was converted to the transient photocharge $Q(t) = CV(t)$.

shown that this optical calibration procedure agrees very well with the total photocharge measured by sweeping carriers out of the electrode gap.[38] The laser intensity was attenuated using neutral density filters to assure that the photocharge response was proportional to the laser intensity. The data reported here were measured with $Q_0 = 1.4 \times 10^{-9}$ C. Several transients were also measured with $Q_0 = 1.4 \times 10^{-10}$ C to verify proportionality.

We used two optical-bias sources. For low optical-bias levels we illuminated the specimen with a light emitting diode ($\lambda \sim 750$ nm). For high bias levels we employed a tungsten halogen bulb (type ENH) without spectral filters. We did not calibrate the flux from these sources. The generation rate was calculated from the dc photocurrent and the mobility-lifetime product obtained from the photocharge transients; the generation rate was varied between 2×10^{17} and 2×10^{21} cm^{-3} s^{-1}.

Finally, we checked that the transients corresponded to the limit of low laser repetition rate. We found it necessary to use a very low pulse repetition rate (less than 0.01 Hz) in some cases before the repetition rate effect was indetectible.

III. EXPERIMENTAL RESULTS

A. Review of the transient photocharge technique

In Fig. 3 we present the transient photocharge measurements without optical bias (lowest curve at 10^{-5} s), and for three successively larger levels of optical bias. The transient photocharge $Q(t)$ is normalized using estimates of the total charge Q_0 of photocarriers generated between the electrodes, the electrode gap d, and the bias voltage V. Note that the dimensions of the normalized photocharge are those of a mobility lifetime product. The dc photocurrents and the corresponding photogeneration rates for each optical-bias level are given in the caption; the procedure for estimating the photogeneration rate will be given shortly.
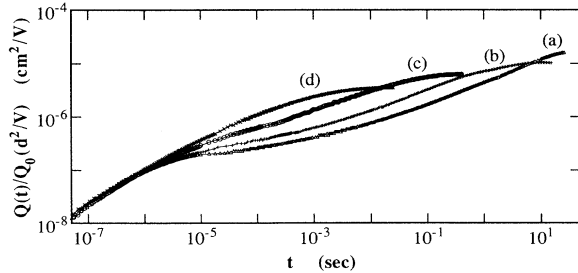
The curve without optical bias is essentially the

FIG. 3. The transient photocharge $Q(t)(d^2/Q_0V)$ recorded at three optical-bias levels and in the dark in an a-Si:H specimen in its annealed state. The dc currents at 100 V bias and the calculated photogeneration rates through the specimen were (a) 2.0×10^{-10} A (dark), (b) 2.4×10^{-9} (2.3×10^{17} cm^{-3}s^{-1}), (c) 2.7×10^{-8} A (3.7×10^{18} cm^{-3}s^{-1}), and (d) 2.4×10^{-7} A (7.6×10^{19} cm^{-3}s^{-1}). Note that optical bias *impedes* deep trapping, thus enhancing electron drift.

same as measured previously.[15] In order to make the present paper reasonably self-contained, we review briefly the interpretation of the normalized transients without bias; additional details may be found in the previous papers.[15,39] We shall assume for undoped a-Si:H that hole motion is negligible on all time scales compared to electron motion. We shall show that this assumption is consistent with our measurements shortly.

The normalization of the photocharge $Q(t)d^2/Q_0V$ can be understood from the observation that $[Q(t)/Q_0]d$ measures the mean displacement $x(t)$ of electrons after their generation at $t = 0$. Since carriers are not swept out of the electrode structure in the present experiments, we expect $x(t)$ to be proportional to the electric field F. We therefore graph the function $x(t)/F = Q(t)d^2/Q_0V$. This function has the dimensions of a mobility-lifetime product, and yields three standard parameters usually obtained by separate measurements.

(1) μ_D. The electron mobility usually estimated using time-of-flight techniques ($\mu_D = L/Ft_T$, where L is the distance traveled and t_T is the transit time) can be obtained as the ratio of $Q(t)(d^2/Q_0V)$ and t. For example, at 100 ns the normalized photocharge is $Q(t)(d^2/Q_0V) \sim 2 \times 10^{-8}$ cm^2/s, yielding a mobility of 0.2 cm^2/V/s. This corresponds to a transit time of 100 ns measured using a structure with a ratio $L/E = 0.2$ cm^2/s of the distance L to the electric field E. The equivalence of the photocharge and the transit time procedures has been demonstrated experimentally in standard time-of-flight structures.[39] For the present case the mobility is somewhat lower than for time-of-flight, for which the electron mobility is typically between 0.5 and 1.0 cm^2/V/s.[6] We have not carefully investigated this difference.

(2) $\mu\tau_{e,r}$. $x(\infty)/F = Q(\infty)d^2/Q_0V$ is essentially the recombination mobility-lifetime product $\mu\tau_{SS}$ usually measured using steady state illumination and the steady state photocurrent i_{SS}; this equivalence has been demonstrated experimentally at elevated temperatures. In Fig. 3 the dark transient is not complete at the longest experimental time of 20 s.[15]

(3) $\mu\tau_{e,t}$. Under near dark conditions, $x(10~\mu s)/F = Q(10~\mu s)d^2/Q_0V$ is the electron deep-trapping mobility-lifetime product $\mu\tau_{e,t}$ usually measured using charge collection in a time-of-flight structure. In Fig. 3 we obtain $\mu\tau_{e,t} = 2 \times 10^{-7}$ cm^2/s, which is a reasonable magnitude for "device-grade" a-Si:H. The equivalence of the transient photocharge technique and of charge collection was demonstrated experimentally in previous work.[38]

Note that the magnitudes for $x(t)/F$ in Fig. 3 are too large to be accounted for by previous estimates for hole motion. In particular, $\mu\tau_{h,r}$ (the recombination mobility-lifetime product for holes) estimated from diffusion length measurements in undoped a-Si:H is of order 10^{-8} cm^2/V.[26,40]

B. Transient measurements with optical bias

The lowest curve (no optical bias) of Fig. 3 shows three of the four domains described in Fig. 1: (i) bandtail transport ($t < 10^{-5}$ s), (ii) a relatively constant, "plateau" region associated with electron deep trapping

(mobility lifetime product $\mu\tau_{e,t} \sim 2 \times 10^{-7}$ cm^2/s), and (iii) further drift following reemission from the deep trap ($t > 10^{-3}$ s). The terminal plateau associated with recombination is not plainly observed in this transient.

The next higher curve was obtained in the presence of optical bias ($i_{SS} = 2.4 \times 10^{-9}$ A). All four features expected from Fig. 1 are discernible. The saturated value of $Q(t)(d^2/Q_0V)$ near 1 s is the incremental recombination mobility-lifetime product $\mu\tau_{e,r} \sim 10^{-5}$ cm^2/V for this bias level. This value is obviously lower than obtained under near dark conditions. This reduction is in agreement with the sublinear dependence of steady-state photocurrents upon incident optical intensity which is typical for a-Si:H.

We can use the value $\mu\tau_{e,r} \sim 10^{-5}$ cm^2/s to roughly estimate the steady-state generation rate G, which is obtained from the steady-state photocurrent i_{SS} as $G = (i_{SS}/eV)(d/wl)(1/\mu\tau_{SS})$. w and l are the width of the electrodes and the specimen thickness, respectively. We approximate $\mu\tau_{SS}$ by $\mu\tau_{e,r}$; the two quantities are exactly equal if $\mu\tau_{e,r}$ is independent of the optical-bias level. We obtain $G \sim 2 \times 10^{17}$ cm^{-3} s^{-1}. This procedure was used to obtain the photogeneration rate estimates given in the figure captions.

The most interesting feature in Fig. 3 is that optical bias *enhances* drift following deep trapping: in the plateau region, $Q(t)(d^2/Q_0V)$ is increased by optical bias. Finally, there is no significant effect of optical bias on the transients before 10^{-6} s. This result indicates that the optical-bias levels used did not affect the fundamental transport mechanism associated with the conduction band tail.

These two trends for optical bias—to accelerate recombination (i.e., to reduce $\mu\tau_{e,r}$), but to suppress deep trapping [i.e., to increase $Q(t)(d^2/Q_0V)$ prior to recombination]—are reasonably clear at the two highest optical-bias levels as well. At the highest optical-bias level in the figure there is no evidence for the characteristic "S" shape in the transient we associate with deep trapping and reemission.

An alternate way for representing these optical-bias effects is to present the transient photocurrent $i(t)$. We computed $i(t)$ numerically for several transients from Fig. 3; the results are presented as Fig. 4. The steepening of the decay near 10^{-6} s for the dark transient is associated with deep trapping. These data are comparable to previous transient photocurrents illustrating deep trapping,[1,15,41] but the range of time is expanded almost a million times. As for the photocharge representation, it is clear that optical bias ultimately eliminates the features in the transient associated with deep-trapping.

In Fig. 5 we present transient photocharge data for two additional, larger values of optical bias ($G > 5 \times 10^{19}$ cm^{-3} s^{-1}). We checked that the sample, which was initially in its annealed state, did not change significantly due to light soaking during the transient measurement. The dominant feature is an additional decrease in the recombination mobility-lifetime product $\mu\tau_{e,r}$; the drift enhancement due to optical bias observed for lower bias levels is not observed at high optical bias.

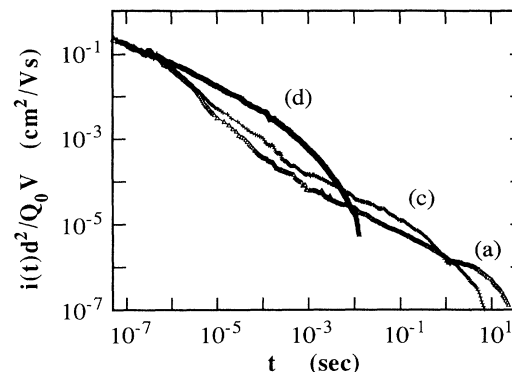We also explored these optical-bias effects in a light-

FIG. 4. Transient photocurrents $i(t)(d^2/Q_0V)$ obtained from differentiation of three photocharge transients of Fig. 3.

soaked state of the specimen. The specimen was illuminated with the unattenuated light from the type ENH tungsten halogen bulb for 70 min. The transient measurements in the low optical-bias region are presented in Fig. 6. By comparison with Fig. 3 for the annealed state, we see that the deep-trapping mobility-lifetime product $\mu\tau_{e,t}$ estimated from the dark transient declined from 2×10^{-7} to about 7×10^{-8} cm^2/V after light-soaking. The steady-state mobility-lifetime product declined about one order of magnitude at a given level of optical bias.

The decrease in $\mu\tau_{e,t}$ makes the "S" shape of the dark transient somewhat more evident than in the annealed state. Optical bias has the same qualitative effects found in the annealed state. In a "low-bias" regime of Fig. 6 the deep-trapping effects are suppressed, leading to an enhancement of electron drift at intermediate time scales. Optical bias diminishes the value of $\mu\tau_{SS}$, but does not affect transport prior to deep trapping. The magnitude of the transients in this early time domain agree fairly well with the transients for the annealed specimen. In Fig. 7 we have presented transient photocurrents corresponding to three of the curves in Fig. 6.

In Fig. 8 we have presented the transient photocharge measurements for high levels of optical bias. The results
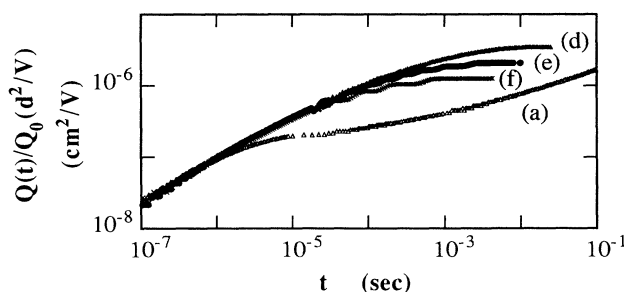

FIG. 5. Additional transient photocharge measurements for the specimen of Fig. 2. The dc photocurrents (and photogeneration rates) were (d) 2.4×10^{-7} A (7.6×10^{19} cm^{-3}s^{-1}), (e) 5.5×10^{-7} A (2.6×10^{20} cm^{-3}s^{-1}), and (f) 1.3×10^{-6} A (1.2×10^{21} cm^{-3}s^{-1}). The lowest curve (a) was measured in the dark.
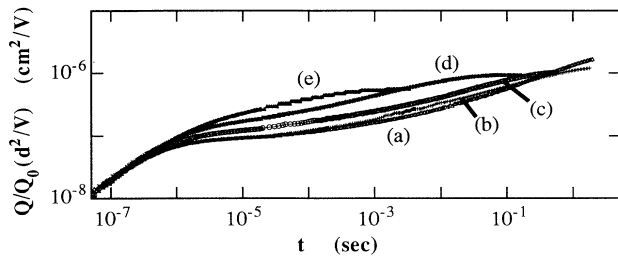
FIG. 6. The transient photocharge $Q(t)(d^2/Q_0V)$ recorded at four optical-bias levels and in the dark in an a-Si:H specimen in a light-soaked state. The dc currents (and photogeneration rates) through the specimen were (a) 5.0×10^{-11} A (dark), (b) 4.8×10^{-10} A $(2.3 \times 10^{17}$ cm^{-3}s$^{-1})$, (c) 1.0×10^{-9} A $(6.3 \times 10^{17}$ cm^{-3}s$^{-1})$, (d) 1.8×10^{-8} A $(1.7 \times 10^{19}$ cm^{-3}s$^{-1})$, and (e) 2.7×10^{-7} A $(4.2 \times 10^{20}$ cm^{-3}s$^{-1})$.
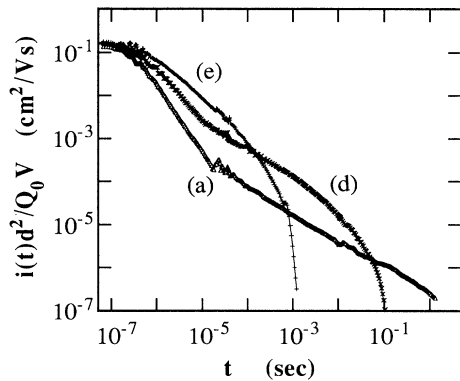

FIG. 7. Transient photocurrents $i(t)(d^2/Q_0V)$ obtained from differentiation of the photocharge data of Fig. 5. For clarity the lowest two optical-bias levels $(1.0 \times 10^{-9}$ and 4.8×10^{-10} A) are omitted.
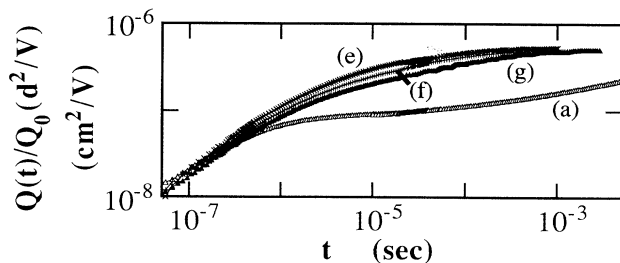

FIG. 8. Additional transient photocharge measurements for the specimen of Fig. 2. The dc photocurrent (and photogeneration rate) were (f) 7.0×10^{-7} A $(1.1 \times 10^{21}$ cm^{-3}s$^{-1})$, and (g) 1.1×10^{-6} A $(1.7 \times 10^{21}$ cm^{-3}s$^{-1})$. Transients (a) and (e) are the same as in Fig. 6.

are qualitatively consistent with the high bias data for the annealed state; the most obvious difference between Fig. 5 and Fig. 8 is that optical bias does not suppress the final, recombination limited value of $Q(t)d^2/Q_0V$ as noticeably in the light-soaked state. This reflects the fact that the photocurrent/generation rate relationship was more nearly linear for the light-soaked state than for the annealed state.

There are also a number of subtle differences between the annealed and light-soaked state which are worth closer examination. In Fig. 9 we have presented the early time region of the transients of Fig. 5 and Fig. 8 on expanded scales. First note the coalescence of the three biased transients onto essentially a single limiting curve in Fig. 9(a) (annealed state). This suggests that the optical-bias suppression of deep trapping has permitted us to observe the fundamental, band-tail domain of transport over about an order of magnitude longer than for the transient without optical bias. The dispersion parameter α which can be extracted from the time dependence $Q(t) \propto t^\alpha$ is about 0.7. This is lower than expected from work on shorter time scales, and suggests that the deep band-tail region for this specimen has a width of about $k_BT/\alpha \sim 35$ meV. In Fig. 9(b) this coalescence is less perfect. We would speculate that the increased recombination rate in the light-soaked specimen caused the optical-bias effect to be less pronounced, and the suppression of deep trapping to be less complete. Finally, in Fig. 9(b) the early time coalescence is not as perfect as for Fig. 9(a), and suggests the possibility of a true, optical-bias-induced change in the band-tail regime; we have not studied this possibility sufficiently to resolve whether systematic errors might account for
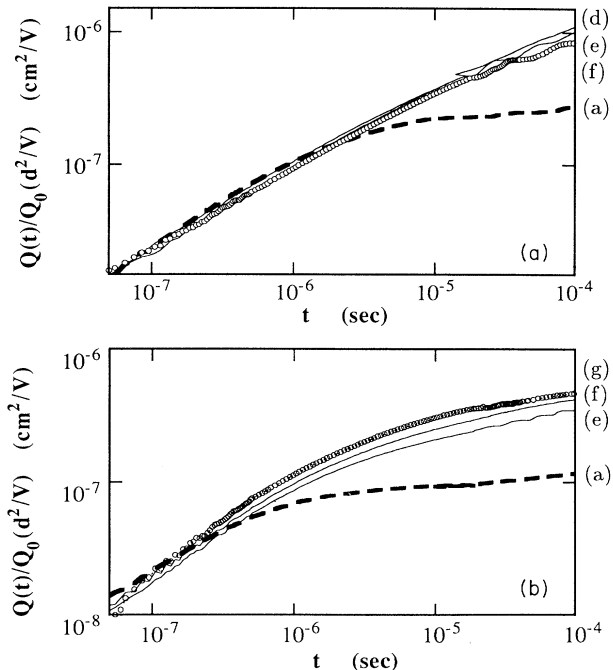

FIG. 9. Transient photocharge measurements for the (A) annealed and (B) light-soaked states. The data are portions of Fig. 5 and Fig. 8 graphed on enlarged scales.

it. Our data also address whether light soaking affects the electron mobility in the band-tail regime. The difference is reasonably small; a more focused discussion of this issue has been given recently by Wang, Antoniadis, and Schiff.[42]

IV. DISCUSSION

A. Comparison with previous optical-bias work

We first compare the present results with previous work on optical bias. Pandya and Schiff[22,23] reported an enhancement of about a factor 3 for electron drift due to optical bias. This is essentially the effect we report in the "low bias" domain. In addition the recombination decay time seen in the transients became much shorter as the optical bias was increased. This latter effect is equivalent to the reduction of the photoconductivity *response time*[16,43] as optical bias increased. This early work was restricted to a relatively small time domain (10^{-5}–10^{-1} s), so the fundamental band-tail domain of transport was not probed.

Ritter, Zeldov, and Weiser[26] measured transient photocurrents under high bias conditions, and observed an exponential decay of the photocurrent in the time domain 100 ns–5 μs. We believe that these results are consistent with our "high bias" data.

Chen and Tai[27] reported an optical-bias enhancement of the photocurrent in the range 1–10 μs of about one order of magnitude. They confirmed the exponential decay noted by Ritter, Zeldov, and Weiser[26] as well as the trend towards shorter decay times with higher bias. We again believe that these results are compatible with those presented here.

In addition to these papers which explicitly addressed optical-bias effects, several reports of *modulated photocurrent* measurements indirectly address them. In the modulated photocurrent technique the specimen is illuminated by a sinusoidally modulated source, and the ac photocurrent in the bias circuit is measured as a function of modulation frequency. Most such measurements have been primarily concerned with estimating the density of trap states in a-Si:H using "phase-shift" or related analyses of the frequency spectrum.[44,11] For a-Si:H measurements at very low illumination levels indicate a trap at 0.6 eV below the conduction band.[9,10,12,45] Measurements at high levels of illumination do not reveal such a trap: the work of Pandya and Schiff was based on modulated photocurrent measurements which were Fourier transformed to obtain the transient photocurrent.[22–25]

The present results improve on these earlier works in two respects. First, the dynamic range is several orders of magnitude larger; it is now clear that optical-bias enhancement of electron drift occurs mainly after electron deep trapping. Second, the present work is calibrated, and yields drift parameters comparable to those obtained using time-of-flight methods. This result confirms that the measurements are primarily sensitive to bulk properties of the material, and are little affected by electrodes or surface inhomogeneities.

B. Relationship to injection measurements

Transient injection currents measured in m-i-n or other structures are a useful alternative to transient photocurrent measurements for estimating electron drift mobilities. In these structures the application of a voltage leads to a transient, space-charge-limited electron current which can be analyzed using procedures[46] (see also Ref. 47) which are very similar to those described above for photocurrents. For a-Si:H estimates of the electron drift mobility from this "single injection" technique near room temperature are comparable to those obtained from photocurrent techniques[28,29] at early times ($t < 10^{-7}$ s). However, the deep trapping process has not been observed, and indeed the long time evolution of the single injection transients depends sensitively on injection level and repetition rate.

An obvious speculation is thus that the transient injection measurements involve an effective excitation which is similar to the effects of optical bias for the photocurrent measurements. Such an effect might be due either to the the pulse repetition rate or to the charge injected in these measurements.

Double injection space-charge-limited transients measured in p-i-n diode structures show an enhancement of the electron drift mobility even in the early time regime[48] which is apparently due to specimen excitation, although we did not find a comparable optical-bias effect. On longer time scales double injection transients are extraordinarily sensitive to repetition rate,[49] which seems to agree qualitatively with the sensitivity of the transient photocurrents both to very low levels of optical bias and to laser repetition rate.

C. Trap distribution estimates

Fourier transform techniques can be used[50,51] to estimate trap distributions from transient photocurrent measurements. The underlying theory is based on the fact that the Fourier transform of a photocurrent transient gives the same frequency spectrum as does a modulated photocurrent measurement.[22,25] This spectrum can be used to determine the effective trap energy distribution[44,11] based on the assumption that the trap emission rate R is related to its energy by $R = \nu \exp(-E/k_B T)$. The analysis is unaffected by "monomolecular" recombination; there has been no serious study of possible artifacts due to "bimolecular" recombination. The density of states yielded by these procedures is instrumentally broadened by a function of width kT.

In Fig. 10 we present a plot of $g(E)$ based on numerical differentiation and Fourier transformation of several transients from Fig. 6. The specific procedure was the following. $\mu(\omega)$ is defined to be the Fourier transform of the normalized transient photocurrent $i(t)d^2/Q_0 V$. The numerical procedures required to compute $\mu(\omega)$ are described elsewhere;[50,51] we note only that conventional fast Fourier transform techniques are unsuitable because
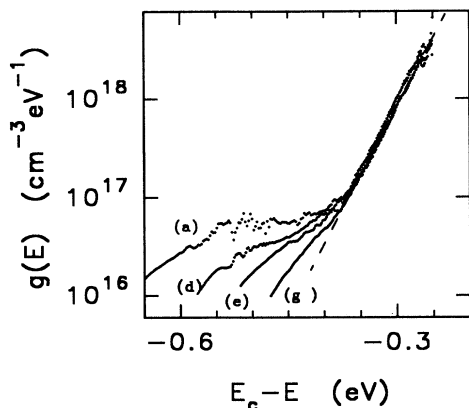
FIG. 10. Trap distribution $g(E)$ estimated by Fourier transformation of the normalized transient photocurrent for (a) near dark conditions and (d), (e), and (g) various intensities of optical bias. The letter codes indicate the conditions presented in Figs. 6–8 (light-soaked state). The dashed line represents a band tail with exponential parameter 28 meV.

of the large dynamic ranges in time which are involved.

To estimate $g(E)$ from $\mu(\omega)$ we used expressions originally proposed in a somewhat different form by Brüggemann et al.:[11]

$$g(E) \sim \frac{2}{\pi k T (b_t/\mu_0)} \mathrm{Im}(1/\mu(\omega)),$$

(1)

$$E = kT \ln(\nu/\omega)$$

b_t/μ_0 (the ratio of a specific trapping rate to the electron mobility) can be assigned the value $b_t/\mu_0 = 10^{-9}$ cm V from previous work correlating deep trapping mobility-lifetime products with the D-center density measured by ESR.[52] We chose a conventional value $\nu_0 = 10^{12}$ s^{-1} to convert the frequency ω to energy units $E = kT \ln(\nu_0/\omega)$ on the horizontal axis. We have shown $g(E)$ for "sensible" ranges $\omega_{BW}/3 > \omega > 10/t_{max}$, where ω_{BW} is the electronic bandwidth of the electronics (120×10^6 s^{-1}) and t_{max} is the longest time recorded in a given transient.

To the right of this plot there is an exponential band tail rising towards the conduction band which appears essentially unchanged by optical bias. The dashed line indicates a characteristic energy E_0 of 28 meV. We have not attempted to correct this value for the 25 meV broadening effect at room temperature; it seems likely that this region is consistent with time-of-flight estimates for the band-tail width of 25 meV or less. We have previously noted that the magnitudes of the measured photocharge are also consistent with time-of-flight work.

Without optical bias the effective density of states has a very broad distribution of deep traps below the band tail. There is no clear peak in the distribution; the shoulder in the distribution to the left (near 0.5 eV) accounts for the typical emission time t_E measured in this sample. Modulated photocurrent measurements under low optical bias often yield a weak peak near 0.6 eV.

Under optical bias the density of traps below the con-

duction band tail is clearly suppressed, consistent with our earlier remarks based on the forms of the transients. The curve at the highest bias level shows only a slight deviation from the exponential band-tail form, appearing essentially as a broadening of the deep band tail. This region accounts for the results shown in Fig. 9(b).

D. Models for optical-bias enhancement

We offer a preliminary discussion of models for the optical-bias enhancement of electron drift after deep-trapping. This is the effect which we consider most remarkable. The increase in the recombination rate under optical bias is well known from steady-state photoconductivity, and is generally attributed to an increase in the recombination center density under optical bias.[16–19]

The two models for optical bias which we have considered are as follows.

(i) Quasi-Fermi-level motion. This is the "conventional" model for excess carrier transport in a-Si:H. An optical-bias enhancement of drift would be due to saturation of the occupancy of the electron deep trap as the steady-state photocurrent is increased.

(ii) Defect relaxation. In the present context this means that the transition energy associated with a specific defect reflects its previous excitation history. An optical-bias enhancement of drift would then require that a given trap site emits an electron considerably faster under optical-bias conditions than in the dark. This suggests that the corresponding level is considerably shallower than in the dark.

A third model—direct photoexcitation of electrons out of their traps by the optical bias—can be rejected for our illumination levels. A typical cross section for optical ionization of defects in a-Si:H is 10^{-16} cm^{-2}.[53] The photon flux required to affect deep trapping in our experiments was less than 10^{14} cm^{-2} s^{-1}. A defect might be optically ionized every 100 s; Fig. 3 shows that the thermal emission rate is thousands of times faster.

We first discuss quasi-Fermi-level motion. To account for electron drift measurements under near dark conditions we use a density of states similar to that of Fig. 1. We consider here only the simplest quasi-Fermi-level model, which assumes that electrons fill the deep traps up to the quasi-Fermi-level. We have illustrated this model in Fig. 11. The upper panel illustrates the occupancy function $f(E)$ in the dark and for several levels of optical bias; the trap occupancy declines steeply (note the logarithmic vertical axis) for energies exceeding the quasi-Fermi-level. The quasi-Fermi-level itself is defined in terms of the ratio of the photocurrent i_P to the dark current i_D: $E_{Fn} - E_F = k_B T \ln(i_P/i_D)$.

The lower panel illustrates the effective density of traps $g(E)$ for a small impulse of electrons excited into the conduction band. The uppermost, limiting curve illustrates $g(E)$ in the dark; this curve essentially reproduces Fig. 1. Under optical bias, the quasi-Fermi-level advances, and the effective density of states becomes $\{1 - f(E)\}g(E)$. It is clear that optical bias can suppress deep trapping by filling the available deep traps, thus leading to the type of drift enhancement we have observed.
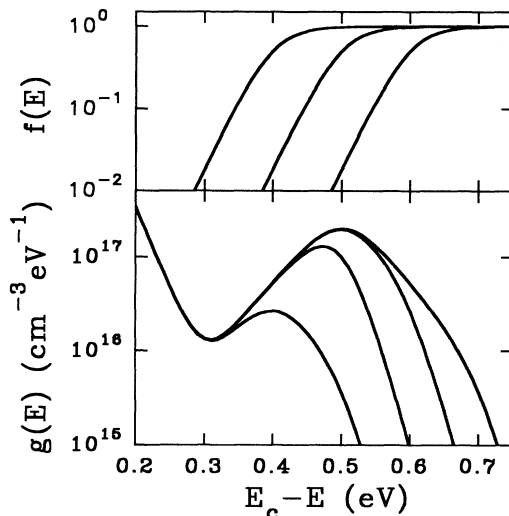
FIG. 11. Effects of quasi-Fermi-level motion on the density of states. The upper panel shows a possible form for the occupancy function of the traps $f(E)$ at three levels of illumination (quasi-Fermi-levels at 0.6, 0.5, and 0.4 eV below the band edge). The lower panel indicates the electron trap distributions which would be probed by transient measurements. The upper curve is the distribution $g(E)$ under thermal equilibrium conditions; the three modified curves show the effects of finite trap occupancy corresponding to the quasi-Fermi-level positions in the upper panel.

Although the quasi-Fermi-level approach may seem promising, it has serious deficiencies as an explanation for the suppression of deep trapping by optical bias. The first of these deficiencies we shall call the "LESR paradox." The electron deep trap in a-Si:H can be identified with near certainty with one of the charge states of the D center in a-Si:H; the density of the neutral charge state of the D center can be measured using electron spin resonance.

If deep trapping is suppressed by quasi-Fermi-level motion, then the density of the corresponding charge state of the D center must also be greatly reduced. For example, if the deep trap is the neutral charge state D^0, then to suppress deep trapping one must entirely suppress the measured spin density. This effect would be readily observable as light induced electron spin resonance (LESR). Alternatively, if most D centers are charged and the deep trap is a D^+, then suppression of deep trapping by the reaction $D^+ + e^- \rightarrow D^0$ would substantially enhance the spin density. Large light induced electron spin resonance effects are in fact observed in a-Si:H, but only at temperatures substantially below those studied here. Near room temperature only very modest light-induced changes in spin density are reported in a-Si:H,[33] which appears to be inconsistent with suppression of deep trapping.

We also suspect that a systematic study of the quasi-Fermi-level model will reveal that suppression of deep trapping occurs with optical-bias levels which are too small to significantly change the density of any charge state of the D center. For example, in Fig. 3 a significant suppression of deep trapping has occurred already when the bias photocurrent is about ten times the dark current, corresponding to only 0.06 eV quasi-Fermi-level shift up from its position in the dark.

Interestingly, although no significant optical-bias effect on the density of spins occurs for a-Si:H near room temperature, a significant decrease of the spin relaxation time of the D center has been reported under illumination.[33,54] This effect was attributed to atomic changes in the defect's structure in response to the continual changes in its charge state under optical excitation, i.e., to a metastable defect configuration. Metastable configurations have also been invoked to account for photocapacitance and capacitance transient measurements;[34-36] from the latter measurements it was inferred that the binding energy of the deep trap increased logarithmically with the length of time the trap had been occupied by an electron.

Based on the density-of-states estimates of Fig. 10, to account for the optical-bias effect using this type of argument, it would be necessary for the deep trap's level to become substantially shallower under optical excitation than in the dark. This view resolves the LESR paradox noted earlier (suppression of deep trapping without a concomitant change in the D-center density). The fact that the trap level shallows under optical bias, and deepens following filling, is an apparent paradox which will be addressed elsewhere.[37]

Once the possibility that the defect energy distribution may be affected by excitation has been acknowledged, many other observations may be viewed as consistent with this effect. An example outside of carrier transport is the intensity shift of the photoluminescence spectrum associated with defects in a-Si:H.[55] The energy of the peak in the defect band photoluminescence shifted from 1.1 to 0.9 eV at 2 K when the intensity of the excitation laser changed from 0.004 to 4 W/cm^2. We shall not discuss detailed luminescence models here, but simply note that this type of shift is certainly compatible with metastable defect configurations.

ACKNOWLEDGMENTS

[1] W. E. Spear and H. L. Steemers, J. Non-Cryst. Solids **66**, 163 (1984).

[2] T. Tiedje, in *Hydrogenated Amorphous Silicon II*, edited by J. D. Joannopoulos and G. Lucovsky (Springer-Verlag, New York, 1984), pp. 261–300.

[3] J. M. Marshall, R. A. Street, and M. L. Thompson, Philos. Mag. B **54**, 51 (1986).

[4] C. E. Nebel and G. H. Bauer, J. Non-Cryst. Solids **114**,

600 (1989).

[5] C. Longeaud and R. Vanderhaghen, Philos. Mag. B **61**, 277 (1990).

[6] Q. Wang, H. Antoniadis, E. A. Schiff, and S. Guha, in *Amorphous Silicon Technology—1992*, edited by M. J. Thompson *et al.*, MRS Symposium Proceedings No. 258 (Materials Research Society, Pittsburgh, 1992), pp. 881.

[7] R. A. Street, Philos. Mag. B **49**, L15 (1984).

[8] S. P. Hotaling, H. Antoniadis, and E. A. Schiff, J. Non-Cryst. Solids **114**, 420 (1989).

[9] H. Oheda *et al.*, Jpn. J. Appl. Phys. **21**, L440 (1982).

[10] G. Schumm and G. H. Bauer, Phys. Rev. B **39**, 5311 (1989).

[11] R. Brüggemann, C. Main, J. Berkin, and S. Reynolds, Philos. Mag. B **62**, 29 (1990).

[12] J. P. Kleider, C. Longeaud, and O. Glodt, J. Non-Cryst. Solids **137&138**, 447 (1991).

[13] K. A. Conrad and E. A. Schiff, Solid State Commun. **60**, 291 (1986).

[14] E. A. Schiff, M. A. Parker, and K. A. Conrad, in *Amorphous Silicon Technology*, edited by A. Madan, M. J. Thompson, P. C. Taylor, P. G. LeComber, and Y. Hamakawa, MRS Symposia Proceedings No. 118 (Materials Research Society, Pittsburgh, 1988), p. 477–488.

[15] H. Antoniadis and E. A. Schiff, Phys. Rev. B **46**, 9482 (1992).

[16] C. R. Wronski and R. E. Daniel, Phys. Rev. B **23**, 794 (1981).

[17] M. Hack and M. Shur, J. Appl. Phys. **58**, 997 (1985).

[18] B. Gu, D. Han, C. Li, and S. Zhao, Philos. Mag. B **53**, 321 (1986).

[19] J. Z. Liu and S. Wagner, Phys. Rev. B **39**, 11 156 (1989).

[20] I. Solomon and R. Benferhat, Phys. Rev. B **30**, 3422 (1984).

[21] F. Schauer, M. Nesladek, and J. Stucklik, Philos. Mag. B **64**, 321 (1991).

[22] R. Pandya and E. A. Schiff, J. Non-Cryst. Solids **59&60**, 297 (1983).

[23] R. Pandya, E. A. Schiff, and K. A. Conrad, J. Non-Cryst. Solids **66**, 193 (1984).

[24] R. Pandya and E. A. Schiff, J. Non-Cryst. Solids **77&78**, 623 (1985).

[25] R. Pandya and E. A. Schiff, Philos. Mag. B **52**, 1075 (1985).

[26] D. Ritter, E. Zeldov, and K. Weiser, Phys. Rev. B **38**, 8296 (1988).

[27] X. Chen and C.-Y. Tai, Phys. Rev. B **40**, 9652 (1989).

[28] E. Snow and M. Silver, J. Non-Cryst. Solids **77&78**, 451 (1985).

[29] D. Han, K. Wang, and M. Silver, J. Non-Cryst. Solids **137&138**, 267 (1991).

[30] H. Antoniadis, Ph.D. thesis, Syracuse University, 1992.

[31] H. Antoniadis and E. A. Schiff, in *Amorphous Silicon Technology — 1990*, edited by P. C. Taylor *et al.*, MRS Sym-

posia Proceedings No. 192 (Materials Research Society, Pittsburgh, 1992), pp. 293–298.

[32] H. Antoniadis and E. A. Schiff, J. Non-Cryst. Solids **137&138**, 435 (1991).

[33] S. Zafar and E. A. Schiff, Thin Solid Films **164**, 239 (1988).

[34] T. M. Leen and J. D. Cohen, J. Non-Cryst. Solids **137&138**, 319 (1991).

[35] T. M. Leen, R. J. Rasmussen, and J. D. Cohen, in *Amorphous Silicon Technology — 1992* (Ref. 6), pp. 211–216.

[36] J. D. Cohen, T. M. Leen, and R. J. Rasmussen, Phys. Rev. Lett. **69**, 3358 (1992).

[37] H. M. Branz and E. A. Schiff, Phys. Rev. B (to be published).

[38] H. Antoniadis and E. A. Schiff, Phys. Rev. B **44**, 3627 (1991).

[39] Q. Wang, H. Antoniadis, E. A. Schiff, and S. Guha, Phys. Rev. B **47**, 9435 (1993).

[40] I. Balberg, in *Amorphous Silicon Technology—1992* (Ref. 6), pp. 693–704.

[41] R. A. Street, Appl. Phys. Lett. **41**, 1060 (1982).

[42] Q. Wang, H. Antoniadis, and E. A. Schiff, Appl. Phys. Lett. **60**, 2791 (1992).

[43] M. A. Parker and E. A. Schiff, in *Materials Issues in Amorphous Semiconductor Technology*, edited by D. Adler, Y. Hamakawa, and A. Madan, MRS Symposia Proceedings No. 70 (Materials Research Society, Pittsburgh, 1986), pp. 125–130.

[44] H. Oheda, J. Appl. Phys. **52**, 6693 (1981).

[45] F. Zhong and J. D. Cohen, in *Amorphous Silicon Technology—1992* (Ref. 6), pp. 813–818.

[46] M. Silver *et al.*, J. Non-Cryst. Solids **66**, 237 (1984).

[47] E. A. Schiff and M. Silver, in *Amorphous Silicon and Related Materials*, edited by H. Fritzsche (World Scientific, Singapore, 1988), pp. 825–851.

[48] M. Silver, G. Winborne, D. Adler, and V. Cannella, Appl. Phys. Lett. **50**, 983 (1987).

[49] D. Han, K. Wang, and M. Silver, in *Amorphous Silicon Technology — 1992* (Ref. 6), pp. 837–842.

[50] C. Main, R. Brüggemann, D. P. Webb, and S. Reynolds, Solid State Commun. **83**, 401 (1992).

[51] D. Melcher and E. A. Schiff (unpublished).

[52] H. Antoniadis and E. A. Schiff, in *Amorphous Silicon Technology—1992* (Ref. 6), pp. 783–788.

[53] W. B. Jackson and N. M. Amer, Phys. Rev. B **25**, 5559 (1982).

[54] R. Pandya, S. Zafar, and E. A. Schiff, in *Materials Issues in Amorphous Semiconductor eechnology* (Ref. 43), pp. 155–159.

[55] D. Han, M. Yoshida, and K. Morigaki, J. Non-Cryst. Solids **97&98**, 651 (1987).